

# Electronic Supporting Information (ESI<sup>+</sup>)

## Aqueous biphasic systems composed of cholinium chloride and polymers as effective platforms for the purification of recombinant green fluorescent protein

Nathalia V. dos Santos<sup>1</sup>, Margarida Martins<sup>2</sup>, Valéria de C. Santos-Ebinuma<sup>1</sup>, Sónia P. M. Ventura<sup>2</sup>, João A. P. Coutinho<sup>2</sup>, Sandro R. Valentini<sup>3</sup>, Jorge F. B. Pereira<sup>1\*</sup>

<sup>1</sup>Department of Bioprocesses and Biotechnology, School of Pharmaceutical Sciences, São Paulo State University (UNESP), Rodovia Araraquara-Jaú/Km 01, 14800-903 – Araraquara, SP, Brazil.

<sup>2</sup> CICECO – Aveiro Institute of Materials, Department of Chemistry, University of Aveiro, 3810-193 Aveiro, Portugal.

<sup>3</sup>Department of Biological Sciences, School of Pharmaceutical Sciences, São Paulo State University (UNESP), Rodovia Araraquara-Jaú/Km 01, 14800-903 – Araraquara, SP, Brazil.

\*Corresponding author

School of Pharmaceutical Sciences, São Paulo State University (UNESP), Rodovia Araraquara-Jaú/Km 01, 14800-903 – Araraquara, SP, Brazil.

Tel: +55 (16) 3301-4675; E-mail address: [jfbpereira@fcar.unesp.br](mailto:jfbpereira@fcar.unesp.br)

**Number of pages: 26.**

**Number of Figures: 11.**

**Number of Tables: 5.**

## Experimental

### Material

Cholinium chloride ([2-hydroxyethyl]trimethylammonium] chloride, [Ch]Cl, purity > 98%), polyethylene glycol with average molecular weight (MW) of 600 g.mol<sup>-1</sup> (PEG-600, pure), 1500 g.mol<sup>-1</sup> (PEG-1500, pure) and 2000 g.mol<sup>-1</sup> (PEG-2000, pure), polypropylene glycol with average MW of 400 g.mol<sup>-1</sup> (PPG-400, pure) and sodium polyacrylate with average MW of 8000 g.mol<sup>-1</sup> (NaPA-8000, 45 wt% in water) were acquired from Sigma-Aldrich® (Brazil) and used as received. The chemical structure of [Ch]Cl and polymers are shown in **Fig. S1**.

The culture media Luria Bertani broth (LB) from Difco and the inductor  $\beta$ -D-1-thiogalactopyranoside (IPTG) from Sigma Aldrich® were used in the fermentative process.

The potassium phosphate buffer was prepared with a mixture of anidre dipotassium hydrogen phosphate (K<sub>2</sub>HPO<sub>4</sub>, 98-100.5%) from QHEMIS and anidre monopotassium hydrogen phosphate (KH<sub>2</sub>PO<sub>4</sub>, 99%) from Synth (Brazil). Tris-HCl buffer at pH 8.0 was prepared with 50 mM of tris(hydroxymethyl)aminomethane in water (Synth, > 99%) and with pH adjustment with hydrochloric acid 37% (HCl, Neon). Milli-Q water (ultrapure water of Type 1) was used in the preparation of all solutions and experiments.

The GFP quantification was done using a Kit K815-100 acquired from BioVision® and used for the determination of GFP calibration curve. Bovine serum albumin (BSA, >98%) used for the total protein calibration curve was commercially obtained from Sigma-Aldrich® (Brazil).

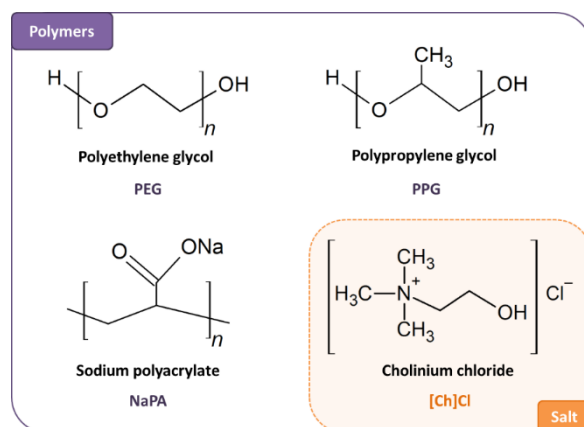


**Fig. S1.** Chemical structure of studied polymers and [Ch]Cl.

### **Bacterial strain and growth conditions for production of GFP**

The plasmid pET28(a) containing the gene for expression of recombinant enhanced GFP (eGFP) was used to transform the host *E. coli* BL21 (DE3) pLysS. The recombinant *E. coli* BL21 (DE3) pLysS was kindly provided by the research group of Prof. Sandro R. Valentini. Initially, the *E. coli* strain was transferred to a Petri dish containing LB agar and IPTG to a final concentration of  $5 \times 10^{-4}$  mol.L<sup>-1</sup>. The antibiotics kanamycin and chloramphenicol (both at 50 µg.mL<sup>-1</sup>) were also added. The plate containing the microorganism was maintained at 37°C for 24 h. Then, a colony was transferred to Erlenmeyer flasks (100 mL) containing 25 mL of LB medium with the antibiotics kanamycin (50 µg.mL<sup>-1</sup>) and chloramphenicol (50 µg.mL<sup>-1</sup>) and incubated overnight at 150 rpm and 37°C, in a refrigerated incubator with orbital shake (TE-421 from Technal, Brazil). Following, Erlenmeyer flasks (500 mL) with 250 mL of fresh LB media were inoculated with 2.5 mL of overnight fermented inoculum [optical density at 600 nm (OD600) of 0.1 Units of Absorbance] The induction with IPTG ( $5 \times 10^{-4}$  mol.L<sup>-1</sup>) occurred after 6 h of incubation and the fermentation process was carried out for more 12 h. The bright green cells (GFP was produced intracellularly) were harvested via centrifugation at 2360 *xg* during 15 min at 4 °C. The pellet containing the cells of *E. coli* was resuspended in 250 mL of cell lysis buffer (Tris-HCl, pH 8.0). The cells were disrupted by the application of four cycles of freezing (-20°C)/thawing (40°C). Then, the insoluble cell components were removed from the supernatant with GFP by centrifugation (15 min at 4°C and 2360 *xg*). The supernatant containing GFP (herein considered as GFP raw extract) was stocked at -20°C before to be used in the extraction and purification experiments. All media were autoclaved at 121°C for 15 min.

### **Determination of GFP 3D fluorescence spectrum and quantification of GFP and Total Protein**

Initially, to find the optimum fluorescence excitation and emission wavelengths from GFP and total protein (TP) of both standards and GFP samples, full 3D fluorescence spectra were acquired at 25°C with a variable wavelength range of excitation from 220-550 nm and emission from 280-560 nm (interval of 2.0 nm for the excitation and emission range) using the spectrofluorophotometer RF-6000 SHIMADZU. With the 3D

spectra, it was possible to observe that both the recombinant GFP samples and the commercial standard [GFP quantification Kit K815-100 (BioVision®)] exhibited similar 3D spectra, in which the maximum GFP fluorescence was obtained with an excitation at 488 nm ( $\lambda_{ex488}$ ) and emission at 510 nm ( $\lambda_{em510}$ ) wavelengths. The maximum fluorescence excitation and emission wavelengths of the protein standard (bovine serum albumin, BSA) were also evaluated and maximum fluorescence was attained with an excitation at 276 nm ( $\lambda_{ex276}$ ) and emission at 336 nm ( $\lambda_{em336}$ ) wavelengths. The peak of fluorescence around 280 nm (indicative of TP) in BSA matched the pattern obtained in the 3D spectra for the recombinant GFP samples regarding TP, suggesting that BSA can be used as a suitable TP standard for GFP, as can be seen in **Fig. S2**. Both GFP and TP fluorescence spectra were not significantly changed neither by the addition of different concentration or by the type of phase-forming agents under study, with all the optimum fluorescence excitation and emission wavelengths stable in all the conditions studied.

Thus, according to the previous 3D fluorescence tests, the calibration curve of GFP concentration *versus* fluorescence intensity at  $\lambda_{ex488}$  and  $\lambda_{em510}$  using the commercial standard GFP was determined at 25°C, and used to determine the GFP concentration of the samples prior and after purification extraction tests. The concentration of TP was also quantified by fluorescence using a calibration curve with BSA as standard, with the TP concentration calibration curve at  $\lambda_{ex276}$  and  $\lambda_{em336}$  at 25°C used to determine the TP composition of each sample. The calibration curves, linear equations and  $R^2$  are presented in **Fig. S3**.

Furthermore, to compare the proportion of GFP over total protein and assess the purity of the GFP, a method using the full 3D fluorescence spectra of purified (phases with high GFP content) and non-purified (GFP raw extract after lysis) samples was developed, comparing the 3D fluorescence spectra of diluted solutions of GFP (GFP concentration equal to  $12.7 \pm 0.2 \text{ mg.L}^{-1}$ ). With that analysis, it was possible to determine the relation between the fluorescence intensity of GFP ( $\lambda_{ex488}$ ,  $\lambda_{em510}$ ) by the fluorescence intensity of TP ( $\lambda_{ex276}$ ,  $\lambda_{em336}$ ), described as GFP/PT (directly proportional to the GFP purity).

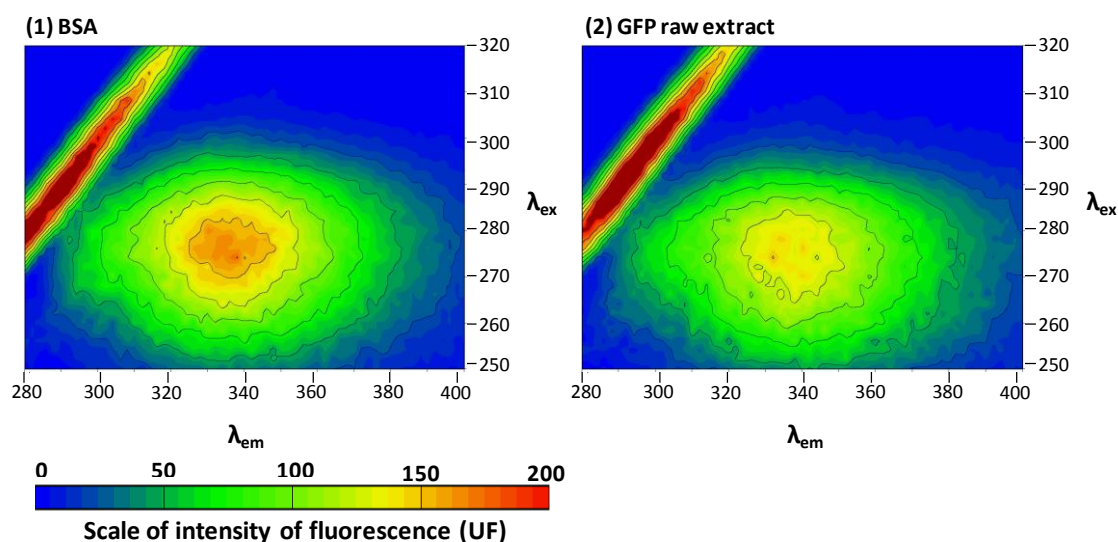


**Fig. S2.** 3D Fluorescence spectra (units of fluorescence, UF) of BSA (1) and GFP raw extract (2). The 3D Fluorescence Spectra shows the excitation wavelengths in the Y axis ( $\lambda_{ex}$ ), the emission wavelengths in the X axis ( $\lambda_{em}$ ) and the intensity of fluorescence is given by the color scale from blue to red (0 to 200 UF). 3D fluorescence spectra ranged excitation wavelength from 250 to 320 nm and emission wavelength from 280 to 400 nm.

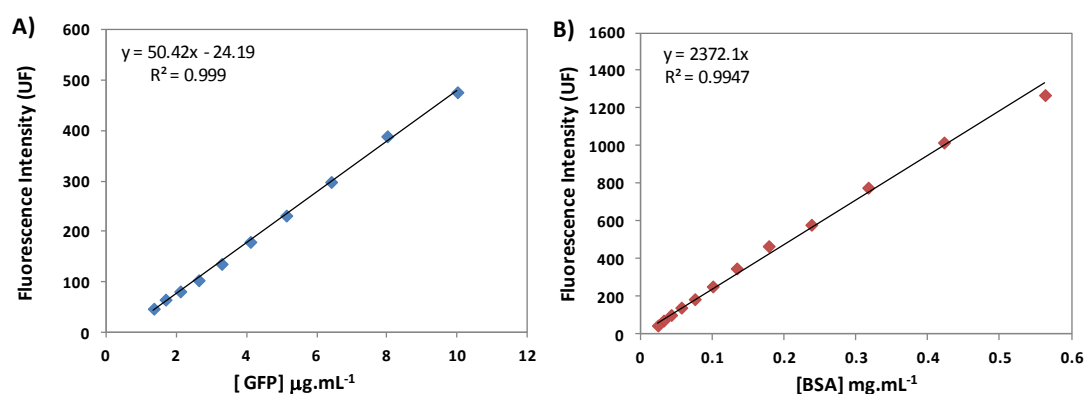


**Fig. S3.** Calibration curves for: A) GFP quantification – with GFP standard (fluorescence analysis at  $\lambda_{Ex488}$   $\lambda_{Em510}$ ); B) Total protein quantification - with BSA as standard (fluorescence analysis at  $\lambda_{Ex276}$   $\lambda_{Em336}$ ).

### Extraction and purification of GFP

The different mixtures for each ABS were prepared adding gravimetrically ( $\pm 10^{-4}$  g) distinct amounts of the respective phase-forming agents (**Table S1**) in 15 mL graduated glass tubes. Then, 10 wt% of GFP raw extract was added and to achieve 5 g (total mass), each system was filled with Milli-Q water. All systems were equilibrated at 25 ( $\pm 1$ )°C during 2 h. The co-existing phases were then carefully separated and characterized for pH, conductivity, viscosity, water content (**Table S2**) and Fourier

transform infrared spectroscopy with an attenuated total reflectance (FTIR-ATR) analysis (Figs. S5 to S8), process detailed in section “Physicochemical characterization of ABS coexisting phases”. All the extraction systems were prepared in triplicate with the respective blank assays carried out to eliminate the interferences of the phase-forming agents or contaminants in the quantification of GFP and TP content. The respective GFP and TP concentrations were measured and SDS-PAGE gel electrophoresis was performed to confirm GFP purification, electrophoresis process described in section “Evaluation of GFP purification by SDS-PAGE”.

The extraction and purification of GFP in each series of ABS was assessed in terms of GFP extraction efficiency ( $EE_{GFP}$ ), GFP mass balance ( $MB_{GFP}$ ) and relative concentration of GFP by total protein ( $[GFP]_{rel}$ ), according to Equations S1 to S3.

**Equations:**

$$EE_{GFP}(\%) = \frac{[GFP]_{GFP\text{-rich phase}} \cdot V_{GFP\text{-rich phase}}}{[GFP]_T \cdot V_T + [GFP]_B \cdot V_B} \times 100 \quad \text{Equation (S1)}$$

where  $V_{GFP\text{-rich phase}}$ ,  $V_0$ ,  $V_T$  and  $V_B$  are the GFP-rich phase, initial top and bottom volumes (mL), and  $[GFP]_{GFP\text{-rich phase}}$ ,  $[GFP]_0$ ,  $[GFP]_T$  and  $[GFP]_B$  represents the GFP-rich phase, initial, top and bottom concentration of GFP ( $g \cdot L^{-1}$ ).

$$MB_{GFP}(\%) = \frac{[GFP]_T \cdot V_T + [GFP]_B \cdot V_B}{[GFP]_0 \cdot V_0} \times 100 \quad \text{Equation (S2)}$$

where  $V_T$ ,  $V_B$  and  $V_0$  are the top, bottom and initial volumes (mL), and  $[GFP]_T$ ,  $[GFP]_B$  and  $[GFP]_0$  represents the top, bottom, and initial concentration of GFP ( $g \cdot L^{-1}$ ).

$$[GFP]_{rel}(\%) = \frac{[GFP]_{GFP\text{-rich phase}}}{[TP]_{GFP\text{-rich phase}}} \times 100 \quad \text{Equation (S3)}$$

where  $[GFP]_{GFP\text{-rich phase}}$  is the concentration of GFP in the GFP rich-phase ( $g \cdot L^{-1}$ ) and  $[TP]_{GFP\text{-rich phase}}$  is the concentration of TP in the GFP rich-phase ( $g \cdot L^{-1}$ ).

**Table S1.** Weight fraction (wt%) composition of the components of each ABS. The references where the phase diagrams are described are also defined.

| Type of ABS   | Weight fraction (wt %) |           |  | Reference        |
|---|------------------------|-----------|--|------------------|
|   | Polymer 1              | Polymer 2 | Buffer or [Ch]Cl   |                  |
| <b>Polymer/Buffer</b>   |                        |           |  |                  |
| PEG-1500 + K <sub>2</sub> HPO <sub>4</sub> /KH <sub>2</sub> PO <sub>4</sub> | PEG-1500               |           | K <sub>2</sub> HPO <sub>4</sub> /KH <sub>2</sub> PO <sub>4</sub> | 1                |
|   | 15                     |           | 15   |                  |
| PEG-2000 + K <sub>2</sub> HPO <sub>4</sub> /KH <sub>2</sub> PO <sub>4</sub> | PEG-2000               |           | K <sub>2</sub> HPO <sub>4</sub> /KH <sub>2</sub> PO <sub>4</sub> | ESI†             |
|   | 15                     |           | 15   |                  |
| <b>Polymer/Polymer + [Ch]Cl as adjuvant</b>                                 |                        |           |  |                  |
| PEG-600/NaPA-8000 + [Ch]Cl  | PEG-600                | NaPA-8000 | [Ch]Cl   | Unpublished data |
|   | 15                     | 15        | 1  |                  |
|   | 15                     | 15        | 3  |                  |
|   | 15                     | 15        | 5  |                  |
|   | 20                     | 15        | 1  |                  |
|   | 20                     | 15        | 3  |                  |
|   | 20                     | 15        | 5  |                  |
| <b>Polymer/[Ch]Cl ABS</b>   |                        |           |  |                  |
| PEG-600/[Ch]Cl  | PEG-600                |           | [Ch]Cl   | 2                |
|   | 38                     |           | 38   |                  |
|   | 40                     |           | 40   |                  |
|   | 42                     |           | 42   |                  |
| PPG-400/[Ch]Cl  | PPG-400                |           | [Ch]Cl   | 3                |
|   | 40                     |           | 10   |                  |
|   | 45                     |           | 12   |                  |
|   | 50                     |           | 14   |                  |

### Determination of relative hydrophobicity of GFP

The relative hydrophobicity of GFP was calculated using the software ProtScale from ExPASy with the Kyte-Doolittle Hydrophilicity plot,<sup>4</sup> considering the protein sequence of the recombinant enhanced GFP (eGFP),<sup>5</sup> and following the equation described by Ishihama *et al.*,<sup>6</sup> defined as:

$$\text{Relative Hydrophobicity in Kyte – Doolite scale} = \frac{\sum_{i=1}^n H_i}{n} \quad \text{Equation (S4)}$$

where  $H_i$  denoted the hydrophobicity value of the amino acid at position  $i$  of a protein of  $n$  amino acids.

### **Physicochemical characterization of ABS coexisting phases**

After the separation of the coexisting phases of each ABS, and considering that the relative densities of both phases were not constant, and thus an inversion of the top and bottom nature phases can occur, their densities were determined. In addition to the densities determination, and to obtain further insights about the characteristics of all systems, pH, conductivity, viscosity, and water content of each coexisting phase were measured (**Table S2**).

The pH values ( $\pm 0.003$ ) and conductivity ( $\pm 1.0\%$  mS.cm<sup>-1</sup>) at 25 ( $\pm 1$ )°C of top and bottom phases for all series of ABS were measured using a portable pH meter and conductometer Metrohm®/Model 914. The calibration of the pH meter was carried out with two standard buffers (pH values of 7.00 and 4.01), while the conductometer was calibrated using a standard solution of KCl (0.1 mol.L<sup>-1</sup>).

Density and viscosity measurements were performed at atmospheric pressure and 25.00 ( $\pm 0.02$ )°C, using an automated SVM 3000 Anton Paar rotational Stabinger viscometer-densimeter. The dynamic viscosities have a relative uncertainty of  $\pm 0.35\%$  while the absolute uncertainty for the density is  $5 \times 10^{-4}$  g.cm<sup>-3</sup>. The viscosimeter was previously calibrated using standard solutions.

The water content of top and bottom phases was measured by volumetric Karl-Fischer titration at 25°C, (except for the NaPA-8000-based ABS, which is incompatible with Karl-Fischer reagents) using a Karl-Fischer 852 Titrand from Metrohm® ( $\pm 0.5\%$ ), HYDRANAL-Methanol Rapid (reagent for accelerated volumetric one component KF titration) and HYDRANAL-Composite 5 (reagent for volumetric one-component Karl Fischer titration methanol free), both reagents supplied by Sigma-Aldrich® as titrants. For the systems containing NaPA-8000, the water content was determined by freeze-drying. Thus, approximately 1 g of each phase of the NaPA-8000-based ABS was freeze-dried for 48 h using the Thermo Scientific ModulyoD Freeze Dryer. After all the water removal, the samples were re-weighted, and the water content was calculated as the percentage of water removed during the freeze-drying process.



Finally, to further confirm the nature of each phase in equilibrium, a Fourier transform infrared spectroscopy with an attenuated total reflectance (FTIR-ATR) analysis of each phase was performed (**Figs. S5 to S8**) and compared with the spectra of pure phase-forming agents (polymers, potassium phosphate buffer or [Ch]Cl). FTIR-ATR spectra were obtained at 25 ( $\pm 1$ )°C using an ALPHA FTIR spectrometer with Platinum ATR single reflection diamond module from Bruker®. The spectra were obtained in the wavelength range from 4000 to 400  $\text{cm}^{-1}$ .

### **Evaluation of GFP purification by SDS-PAGE**

To further confirm the GFP purification obtained after each step of the integrated process developed in this work, sodium dodecyl sulfate polyacrylamide gel electrophoresis (SDS-PAGE) was performed using a Mini-PROTEAN® III (Bio-Rad®) System (BioRad, Brazil). The standard for SDS-PAGE was the PageRuler Prestained Protein Ladder 10 to 180 kDa (Thermo Fisher®). All reagents for the electrophoresis were obtained from Bio-Rad® or Sigma-Aldrich®. Some of the phase-forming agents used in the ABS interfere with the electrophoresis run, and therefore, those were removed using the Vivaspin® 20 10 kDa centrifugal concentrators. All samples, including the GFP raw extract, were subjected to the removal of solvents using the centrifugal concentrators and centrifugation at 4°C and 8000  $\times g$  for 45 min. It is important to note that only components with a molecular weight lower than 10 kDa were removed in the collector, and thus, all the protein content (GFP and contaminants) of the samples were recovered in the concentrator (the ladder standard for SDS-PAGE starts from 10 kDa). Protein SDS-PAGE was then performed as described by Sambrook and Russell.<sup>7</sup> The standard (4  $\mu\text{L}$ ) was loaded in one well of the gel [10% resolving gel and 5% stacking gel (wt/v%), 1 mm thickness], and in the other wells, samples with 15  $\mu\text{g}$  of GFP were added after 10 min incubation at 96°C with Laemli Buffer 2X with 0.2 mol.L<sup>-1</sup> dithiothreitol (DTT). The initial voltage of the electrophoresis was 80 V (during stacking) and 120 V (during the resolving phase). The gel was revealed with Coomassie Blue R solution.

### **Back-Extraction of GFP**

Back-extraction was applied to possibly increase the purification capacity of the systems by integrating two ABS that exhibited good extraction efficiencies but low GFP purification aptitudes. Thus, the PEG-rich phase (containing the GFP) recovered after a first extraction using ABS composed of 15 wt% of PEG-600, 15 wt% of NaPA-8000, and 3 wt% of [Ch]Cl was introduced in a second extraction unit based on a PEG-600/[Ch]Cl ABS (additional content of PEG-600 and [Ch]Cl were added to form a biphasic system with 5 g). After the second extraction stage, the phases were carefully separated and the extraction and purification parameters calculated as previously described in **section “Extraction and purification of GFP”**. The back-extraction procedures were performed in triplicate with the respective blanks to eliminate errors in the quantification.

### **Solvent recycling and GFP polishing**

The ABS allowing the highest purification yield, namely PPG-400/[Ch]Cl-based ABS, was chosen to be integrated with an ultrafiltration unit to attempt at the solvent recycling and GFP polishing. Thus, a system (10 g of total mass) composed of 45 wt% of PPG-400 and 12 wt% of [Ch]Cl was prepared as previously described in **section “Extraction and purification of GFP”** (in triplicate with a blank, to subtract interferences). Similarly, after the extraction and separation of the two co-existing phases, the GFP and TP concentration were measured and the corresponding extraction and purification parameters properly determined. Then, each of the co-existing phases was subjected to a further ultrafiltration to remove the contaminants, GFP polishing and the solvent recycling. The ultrafiltration using Vivaspin® 20 10 kDa centrifugal concentrators (from GE Healthcare, Brazil) associated with a centrifugation process at 4°C and 8000 xg for 45 min was applied to separate the protein contaminants (molecular weight above 10 kDa) from the top PEG-rich phase and to allow the recovery of GFP from the [Ch]Cl-rich aqueous rich phase (GFP polishing). The Vivaspin® 20 10 kDa contains up to 15 mL of sample and, after the centrifugation, 1 mL of a concentrated aqueous solution containing the proteins (GFP or contaminants) was recovered in the retentate (in the concentrator tube), while the solvents were recovered in the permeate (in the collector tube coupled bellow the concentrator).

Each of the co-existing phases was added to the centrifugal concentrators, which were filled with 1 mL of Milli-Q water, and then subjected to the centrifugation. After that, for the tubes containing the PPG-400-rich phase (top phase), the retentate solution containing the contaminant proteins was discarded, and the permeate aqueous solution rich in PPG-400 was recycled. On the other hand, both retentate and permeate aqueous solutions of the [Ch]Cl-rich phase (bottom phase containing the pure GFP) were carefully recovered. The aqueous solution containing the concentrated and pure GFP (retentate) was used for the analysis of extraction and purity yields, while the diluted [Ch]Cl-rich phase, without GFP and recovered as permeate, was recycled in the extraction unit. The recycled phases were then weighted, with the adjustment of phase-forming agents' concentration, and then mixed at 25°C with 10 wt% of GFP raw extract for the formation of a new ABS (details related to the phases weight recovered are compiled in **Table S5**). Again, the phases were separated and the corresponding GFP extraction and purification parameters determined.

## Physical chemical characterization, extraction and purification parameters

**Table S2.** Detailed weight fraction compositions, physicochemical characteristics [pH, conductivity ( $\text{mS cm}^{-1}$  at  $25^\circ\text{C}$ ), viscosity (mPa S), density ( $\text{g cm}^{-3}$ ), water content (wt%)],  $\text{EE}_{\text{GFP}}$  (%),  $\text{MB}_{\text{GFP}}$  (%) and  $[\text{GFP}]_{\text{rel}}$  (%) (with respective standard deviations) of each ABS.

| ABS  | Weight fraction (wt%) |                    |  | pH   |        | Conductivity ( $\text{mS cm}^{-1}$ $25^\circ\text{C}$ ) |        | Viscosity (mPa S) |         | Density ( $\text{g cm}^{-3}$ ) |        | Water content (wt%) |        | $\text{EE}_{\text{GFP}}$ (%) | $\text{MB}_{\text{GFP}}$ (%) | $[\text{GFP}]_{\text{rel}}$ (%) <sup>*</sup> |
|--|-----------------------|--------------------|--|------|--------|---|--------|-------------------|---------|--------------------------------|--------|---------------------|--------|------------------------------|------------------------------|--|
|  | Polymer 1             | Polymer 2          | Buffer or salt   | Top  | Bottom | Top   | Bottom | Top               | Bottom  | Top                            | Bottom | Top                 | Bottom |                              |                              |  |
| Polymer/Polymer with [Ch]Cl as adjuvant ABS                | PEG-600 (Top)         | NaPA-8000 (Bottom) | [Ch]Cl   |      |        |   |        |                   |         |                                |        |                     |        | Top Phase (PEG-600)          |                              |  |
|  | 15.156                | 15.226             | 1.024  | 7.66 | 7.97   | 7.34  | 49.41  | 5.037             | 37.326  | 1.0613                         | 1.1890 | 67.11               | 68.21  | $99.32 \pm 0.01$             | $91.4 \pm 1.6$               | $73.9 \pm 2.0$                               |
|  | 15.010                | 15.026             | 3.042  | 7.92 | 7.99   | 13.67   | 47.25  | 4.907             | 46.882  | 1.0637                         | 1.1943 | 65.12               | 66.66  | $99.30 \pm 0.06$             | $90.7 \pm 1.6$               | $73.3 \pm 5.8$                               |
| PEG-600/NaPA-8000 + [Ch]Cl                                 | 15.561                | 14.984             | 5.055  | 7.89 | 7.94   | 18.25   | 45.05  | 5.415             | 58.733  | 1.0694                         | 1.2016 | 63.25               | 64.55  | $99.32 \pm 0.07$             | $93.0 \pm 1.1$               | $70.0 \pm 2.5$                               |
|  | 20.035                | 15.211             | 1.006  | 7.70 | 7.48   | 4.61  | 44.70  | 7.182             | 113.960 | 1.0760                         | 1.2324 | 59.68               | 63.87  | $99.38 \pm 0.04$             | $103.1 \pm 1.0$              | $73.1 \pm 6.3$                               |
|  | 20.224                | 15.206             | 3.085  | 7.30 | 7.02   | 9.74  | 43.38  | 6.826             | 94.529  | 1.0734                         | 1.2217 | 59.52               | 63.36  | $99.44 \pm 0.05$             | $106.6 \pm 3.5$              | $70.5 \pm 3.7$                               |
|  | 20.133                | 15.360             | 5.081  | 7.39 | 7.44   | 13.40   | 42.05  | 7.807             | 89.989  | 1.0787                         | 1.2187 | 55.76               | 60.12  | $99.41 \pm 0.01$             | $102.8 \pm 3.9$              | $68.9 \pm 2.8$                               |
| Polymer/Buffer ABS   | PEG-1500 (Top)        | -                  | $\text{K}_2\text{HPO}_4/\text{KH}_2\text{PO}_4$ (Bottom) |      |        |   |        |                   |         |                                |        |                     |        | Top phase (PEG-1500)         |                              |  |
| PEG-1500 + $\text{K}_2\text{HPO}_4/\text{KH}_2\text{PO}_4$ | 15.020                | -                  | 14.957   | 6.82 | 6.60   | 6.74  | 122.30 | 10.513            | 2.033   | 1.0876                         | 1.1984 | 64.58               | 71.63  | $98.89 \pm 0.07$             | $91.67 \pm 3.9$              | $73.9 \pm 3.6$                               |
| Polymer/Buffer ABS   | PEG-2000 (Top)        | -                  | $\text{K}_2\text{HPO}_4/\text{KH}_2\text{PO}_4$ (Bottom) |      |        |   |        |                   |         |                                |        |                     |        | Top Phase (PEG-2000)         |                              |  |
| PEG-2000 + $\text{K}_2\text{HPO}_4/\text{KH}_2\text{PO}_4$ | 14.963                | -                  | 14.949   | 6.88 | 6.62   | 5.35  | 124.40 | 14.778            | 1.875   | 1.0856                         | 1.1959 | 75.40               | 78.85  | $98.81 \pm 0.05$             | $92.61 \pm 4.0$              | $74.8 \pm 2.3$                               |

\*GFPrel (%) of extract -  $69.7 \pm 0.1$  %.

**Table S2.** Continued.

| ABS                        | Weight fraction (wt%) |   |                    | pH   |        | Conductivity (mS cm <sup>-1</sup> 25° C) |        | Viscosity (mPa S) |         | Density (g cm <sup>-3</sup> ) |        | Water content (wt%) |        | EE <sub>GFP</sub> (%)    | MB <sub>GFP</sub> (%)   | [GFP] <sub>rel</sub> (%) <sup>*</sup> |
|----------------------------|-----------------------|---|--------------------|------|--------|--|--------|-------------------|---------|-------------------------------|--------|---------------------|--------|--------------------------|-------------------------|---------------------------------------|
|                            | Polymer 1             | Polymer 2                                       | Buffer or salt     | Top  | Bottom | Top                                      | Bottom | Top               | Bottom  | Top                           | Bottom | Top                 | Bottom |                          |                         |                                       |
| Polymer/[Ch]Cl<br>ABS      | PEG-600<br>(Bottom)   | -   | [Ch]Cl (Top)       |      |        |  |        |                   |         |                               |        |                     |        | Top Phase<br>([Ch]Cl)    |                         |                                       |
|                            | 38.325                | -   | 37.807             | 6.12 | 5.66   | 31.72                                    | 0.53   | 15.738            | 100.840 | 1.0942                        | 1.1202 | 33.08               | 14.81  | 99.32 ± 0.08             | 96.3 ± 6.4              | 80.1 ± 5.4                            |
| PEG-600/[Ch]Cl             | 39.919                | -   | 40.081             | 6.01 | 6.25   | 37.31                                    | 0.30   | 14.948            | 115.210 | 1.0927                        | 1.1209 | 31.65               | 12.41  | 99.09 ± 0.06             | 91.4 ± 4.3              | 78.6 ± 8.3                            |
|                            | 41.940                | -   | 41.955             | 5.79 | 6.01   | 31.32                                    | 0.13   | 18.232            | 118.290 | 1.0956                        | 1.1215 | 29.14               | 12.31  | 99.00 ± 0.06             | 84.9 ± 6.3              | 78.1 ± 5.9                            |
| PPG-400/[Ch]Cl             | PPG-400<br>(Top)      | -   | [Ch]Cl<br>(Bottom) |      |        |  |        |                   |         |                               |        |                     |        | Bottom Phase<br>([Ch]Cl) |                         |                                       |
|                            | 40.342                | -   | 9.967              | 5.33 | 5.53   | 0.59                                     | 26.70  | 55.770            | 4.667   | 1.0273                        | 1.0341 | 24.70               | 62.46  | 99.52 ± 0.03             | 90.1 ± 3.7              | 93.2 ± 5.9                            |
| PPG-400/[Ch]Cl             | 45.548                | -   | 11.933             | 5.62 | 5.83   | 0.30                                     | 45.60  | 63.100            | 3.425   | 1.0250                        | 1.0362 | 16.86               | 63.15  | 99.01 ± 0.05             | 91.8 ± 3.0              | 100.2 ± 3.5                           |
|                            | 49.973                | -   | 14.066             | 5.47 | 5.87   | 0.14                                     | 64.21  | 69.200            | 3.047   | 1.0222                        | 1.0460 | 13.06               | 56.44  | 98.53 ± 0.10             | 89.2 ± 1.8              | 97.8 ± 1.4                            |
| Back-extraction<br>ABS     | PEG-600<br>(Top)      | NaPA-8000<br>(Bottom)                           | [Ch]Cl             |      |        |  |        |                   |         |                               |        |                     |        | Top Phase<br>(PEG-600)   |                         |                                       |
| 1 <sup>st</sup> extraction | 14.923                | 14.975  | 3.054              | 7.75 | 7.57   | 12.99                                    | 39.50  | 5.002             | 54.595  | 1.0644                        | 1.1997 | 65.49               | 66.83  | 99.40 ± 0.05             | 96.9 ± 2.8              | 71.4 ± 5.7                            |
| 2 <sup>nd</sup> extraction | PEG-600<br>(Bottom)   | Top phase<br>from 1 <sup>st</sup><br>extraction | [Ch]Cl (Top)       |      |        |  |        |                   |         |                               |        |                     |        | Top Phase<br>([Ch]Cl)    |                         |                                       |
|                            | 25.269                | 32.26   | 34.878             | 8.18 | 7.92   | 28.24                                    | 0.57   | 17.419            | 74.920  | 1.1003                        | 1.128  | 30.11               | 18.46  | 99.60 ± 0.01             | 88.6 ± 1.2 <sup>#</sup> | 99.8 ± 3.7                            |

<sup>\*</sup>GFPrel (%) of extract - 69.7 ± 0.1 %.

<sup>#</sup>MB considering initial GFP mass (overall MB considering 1<sup>st</sup> and 2<sup>nd</sup> extractions).

## Phase diagram determination

The ternary phase diagram for the PEG-2000 + K<sub>2</sub>HPO<sub>4</sub>/KH<sub>2</sub>PO<sub>4</sub> ABS was determined at 298 (±1) K and at atmospheric pressure (**Table S3**), by the cloud point titration method.<sup>8</sup> Aqueous solutions of PEG-2000 at ≈ 60 wt% and aqueous solutions of the buffer K<sub>2</sub>HPO<sub>4</sub>/KH<sub>2</sub>PO<sub>4</sub> (pH 7; ≈ 40 wt%) were prepared and used for the determination of the binodal curves of the polymeric systems. The system compositions were determined by the weight quantification of all components added within ± 10<sup>-4</sup> g. The experimental binodal curves (in weight fraction percentage) were correlated using the Merchuk equation,<sup>9</sup> described as follows:

$$Y = A \times \exp[(BX^{0.5}) - (CX^3)] \quad \text{Equation (S5)}$$

where Y and X, represent PEG and inorganic salt weight percentages, respectively. A, B and C are constants obtained by the regression of the experimental binodal data.

In the studied ABS, the top phase corresponded to the PEG-rich phase, while the bottom phase was mainly composed by the phosphate-buffer (considering the FT-IR from **Fig. S6** and conductivity and viscosity from **Table S2** – PEG phase have lower values for conductivity and higher values for viscosity, and also have a more similar pattern to the PEG standard in the FT-IR spectra). The experimental binodal data was fitted by the empirical relationship described by Equation (S5). The regression parameters were estimated by the least-squares regression, and their values and corresponding standard deviations were  $90.36 \pm 2.22$ ,  $-0.511 \pm 0.012$  and  $2.684 \times 10^{-4} \pm 1.96 \times 10^{-5}$  for A, B and C, respectively. In general, a good correlation between the experimental data and the parameters was obtained ( $R^2 = 0.9967$  and mean squared deviation = 0.35935), indicating that these fittings can be used to predict data in a specific region of the phase diagram where no experimental data are available, as described in **Fig. S4**.

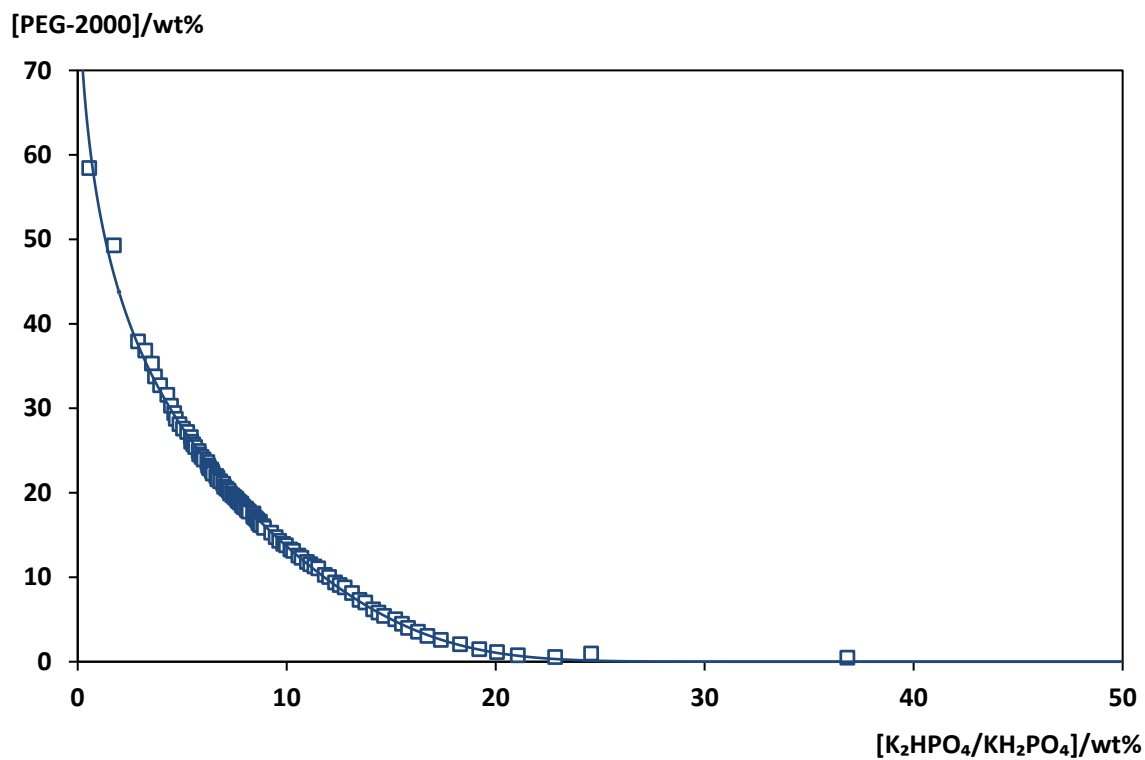


**Fig. S4.** Binodal curve for the ternary systems composed of PEG-2000 + K<sub>2</sub>HPO<sub>4</sub>/KH<sub>2</sub>PO<sub>4</sub> (pH 7) + H<sub>2</sub>O, at 298 (±1) K.

**Table S3.** Weight fraction (w, wt%) data for the ternary systems composed of PEG-2000 (1) + K<sub>2</sub>HPO<sub>4</sub>/KH<sub>2</sub>PO<sub>4</sub> (2) + H<sub>2</sub>O (3) at 25°C and pH 7.

| w1       | w2       |  | w1       | w2       |  | w1       | w2       |
|----------|----------|--|----------|----------|--|----------|----------|
| 58.42437 | 0.562859 |  | 21.06194 | 6.972367 |  | 13.27194 | 10.18537 |
| 49.26235 | 1.742253 |  | 20.68231 | 7.017107 |  | 13.09396 | 10.31974 |
| 37.89252 | 2.901231 |  | 20.46833 | 7.123536 |  | 12.54766 | 10.57263 |
| 36.81171 | 3.238451 |  | 20.24508 | 7.234466 |  | 12.29095 | 10.71429 |
| 35.26683 | 3.567477 |  | 19.90789 | 7.301978 |  | 11.78791 | 10.97369 |
| 33.75769 | 3.712223 |  | 19.66289 | 7.415254 |  | 11.51793 | 11.13575 |
| 32.69948 | 3.956477 |  | 19.46818 | 7.515810 |  | 11.25842 | 11.33941 |
| 31.57079 | 4.298149 |  | 19.26964 | 7.596715 |  | 11.02314 | 11.52046 |
| 30.27585 | 4.478772 |  | 19.04345 | 7.658419 |  | 10.26256 | 11.83541 |
| 29.41505 | 4.627360 |  | 18.87769 | 7.744907 |  | 10.00918 | 12.04028 |
| 28.72553 | 4.706418 |  | 18.70314 | 7.834514 |  | 9.360700 | 12.32877 |
| 28.10760 | 4.879526 |  | 18.46185 | 7.875029 |  | 9.052108 | 12.54371 |
| 27.58184 | 5.046982 |  | 18.29381 | 7.951765 |  | 8.780667 | 12.78578 |
| 27.16746 | 5.244942 |  | 18.10748 | 8.069320 |  | 8.108906 | 13.13353 |
| 26.57263 | 5.423158 |  | 17.89441 | 8.121810 |  | 7.300127 | 13.49782 |
| 26.01723 | 5.438430 |  | 17.75196 | 8.194425 |  | 6.992313 | 13.77098 |
| 25.72244 | 5.538211 |  | 17.52374 | 8.420059 |  | 6.188999 | 14.14568 |
| 25.40149 | 5.634937 |  | 17.22858 | 8.414731 |  | 5.797979 | 14.40041 |
| 24.92791 | 5.800055 |  | 17.11272 | 8.436237 |  | 5.405427 | 14.67220 |
| 24.52302 | 5.819312 |  | 16.98194 | 8.500928 |  | 4.997708 | 15.20160 |
| 24.21626 | 5.938375 |  | 16.85450 | 8.567461 |  | 4.474634 | 15.52588 |
| 23.90893 | 6.038794 |  | 16.72364 | 8.614357 |  | 3.981884 | 15.81832 |
| 23.61018 | 6.214740 |  | 16.57257 | 8.723510 |  | 3.533446 | 16.29567 |
| 23.21415 | 6.253219 |  | 16.39647 | 8.655755 |  | 3.034510 | 16.74112 |
| 23.03537 | 6.275140 |  | 16.28267 | 8.730875 |  | 2.556691 | 17.38679 |
| 22.90162 | 6.302573 |  | 16.15719 | 8.742448 |  | 2.048639 | 18.30308 |
| 22.71288 | 6.401785 |  | 16.01330 | 8.887874 |  | 1.467205 | 19.22625 |
| 22.49670 | 6.436388 |  | 15.82061 | 8.927327 |  | 1.125973 | 20.07612 |
| 22.23906 | 6.471210 |  | 15.26308 | 9.266025 |  | 0.747296 | 21.07214 |
| 21.95894 | 6.641614 |  | 14.71845 | 9.480480 |  | 0.538774 | 22.85190 |
| 21.75007 | 6.692859 |  | 14.29278 | 9.655835 |  | 0.957874 | 24.57909 |
| 21.55985 | 6.695819 |  | 13.92618 | 9.842041 |  | 0.459675 | 36.83897 |
| 21.34619 | 6.828344 |  | 13.76840 | 9.976558 |  |          |          |



## ABS' phases FTIR-ATR analysis

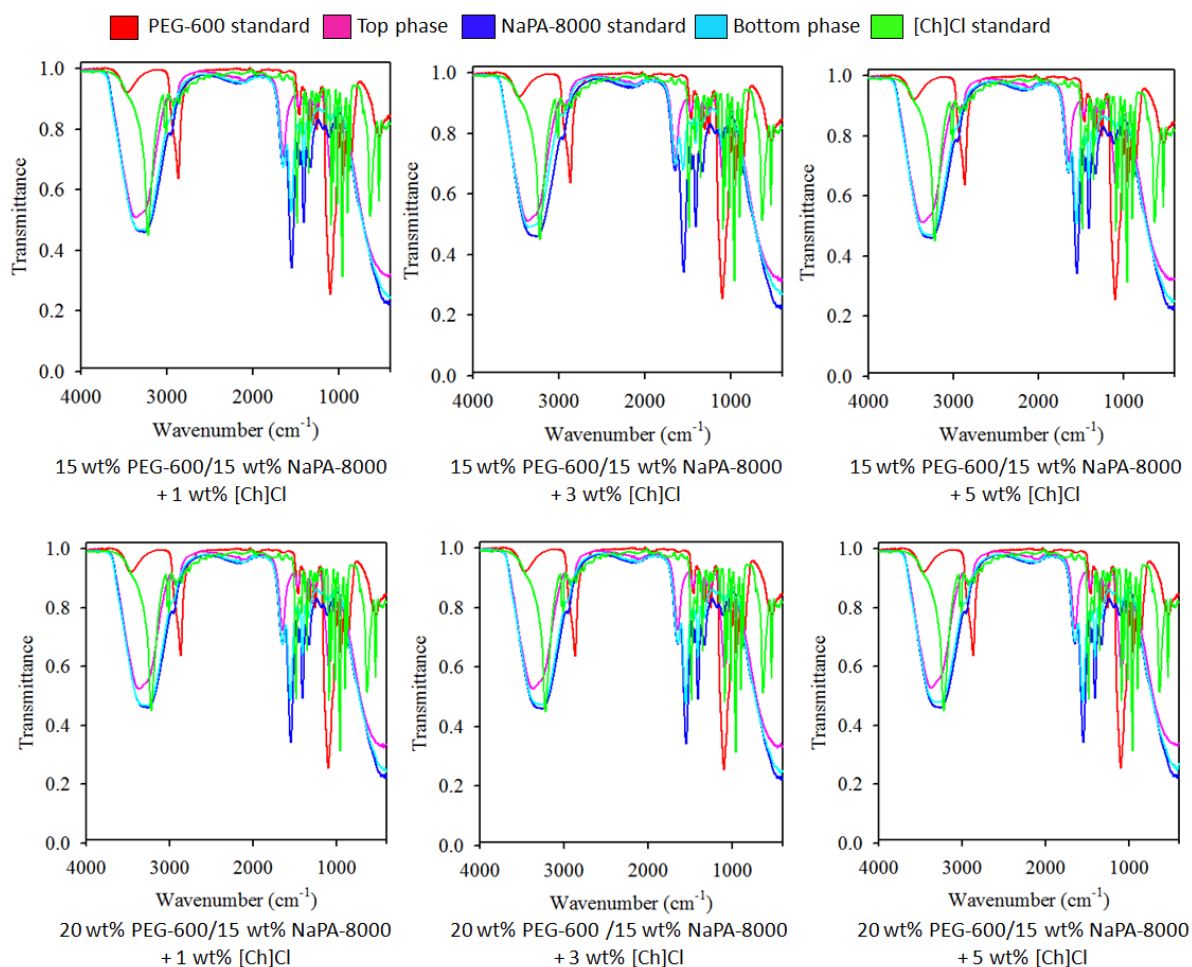


**Fig. S5.** Fourier transform infrared spectroscopy with an attenuated total reflectance (FTIR-ATR) of top (pink) and bottom (light blue) phases from ABS composed of PEG-600 (15 or 20 wt%) + NaPA-8000 (15 wt%) + [Ch]Cl (1, 3 or 5 wt%), and standards for PEG-600 (red), NaPA-8000 (blue) and [Ch]Cl (green). Wavenumber ( $\text{cm}^{-1}$ ) in the x axis and transmittance in the y axis.

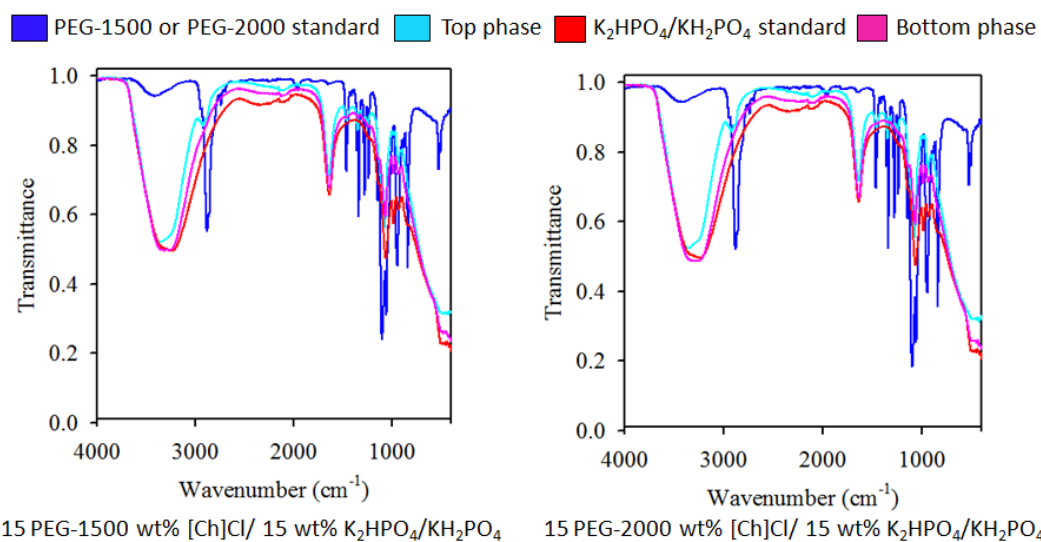


**Fig. S6.** Fourier transform infrared spectroscopy with an attenuated total reflectance (FTIR-ATR) of top (pink) and bottom (light blue) phases from ABS composed of PEG-1500 (15 wt%) +  $K_2HPO_4/KH_2PO_4$  (15 wt%) and PEG-2500 (15 wt%) +  $K_2HPO_4/KH_2PO_4$ , and standards for PEG-1500 or PEG-2000 (red) and  $K_2HPO_4/KH_2PO_4$  (blue). Wavenumber ( $cm^{-1}$ ) in the x axis and transmittance in the y axis.

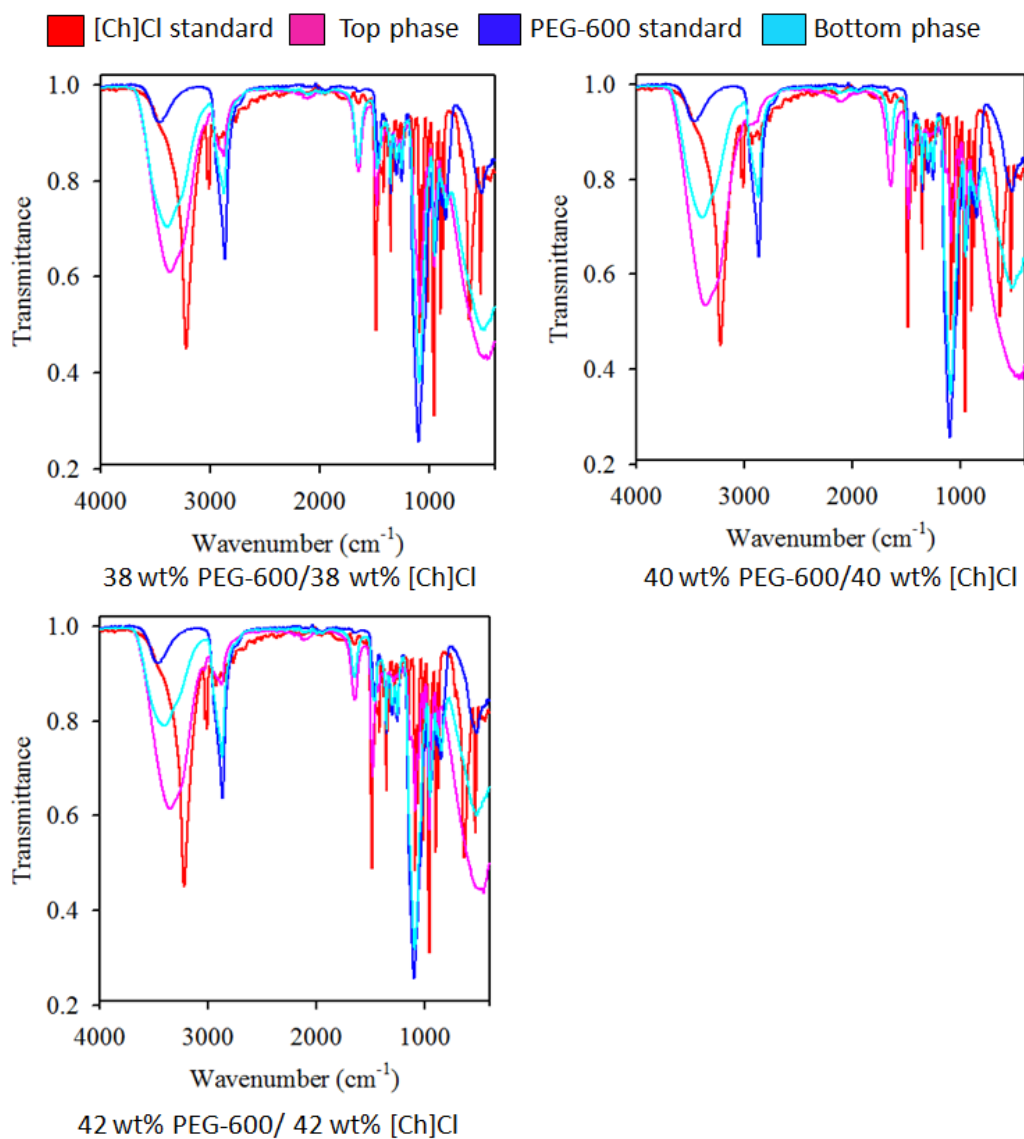


**Fig. S7.** Fourier transform infrared spectroscopy with an attenuated total reflectance (FTIR-ATR) of top (pink) and bottom (light blue) phases from ABS composed of PEG-600 (38, 40 or 42 wt%) and [Ch]Cl (38, 40 or 42 wt%), and standards for [Ch]Cl (red) and PEG-600 (blue). Wavenumber ( $\text{cm}^{-1}$ ) in the x axis and transmittance in the y axis.

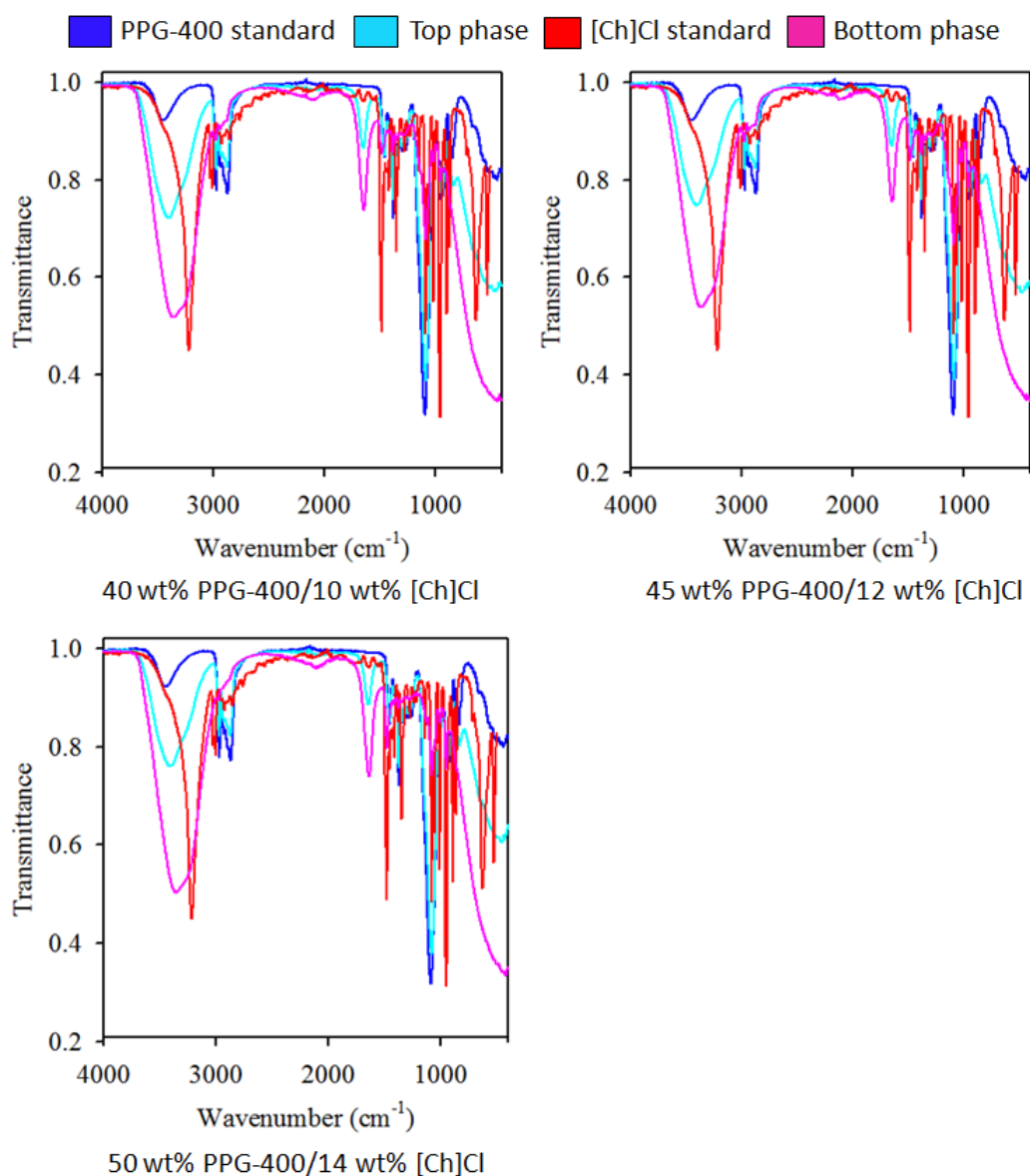


**Fig. S8.** Fourier transform infrared spectroscopy with an attenuated total reflectance (FTIR-ATR) of top (light blue) and bottom (pink) phases from ABS composed of PPG-400 (40, 45 or 50 wt%) and [Ch]Cl (10, 12 and 14 wt%), and standards for [Ch]Cl (red) and PPG-400 (blue). Wavenumber ( $\text{cm}^{-1}$ ) in the x axis and transmittance in the y axis.

## Extraction and purification of GFP

### 1<sup>st</sup> Purification step

PEG-600/NaPa-8000 + [Ch]Cl ABS

$EE_{GFP} = 99.40 \pm 0.05 \%$  /  $MB_{GFP} = 96.9 \pm 2.8\%$

### 2<sup>nd</sup> Purification step

PEG-600/[Ch]Cl ABS

$EE_{GFP} = 99.60 \pm 0.01\%$  /  $MB_{GFP} = 88.6 \pm 1.2\%$

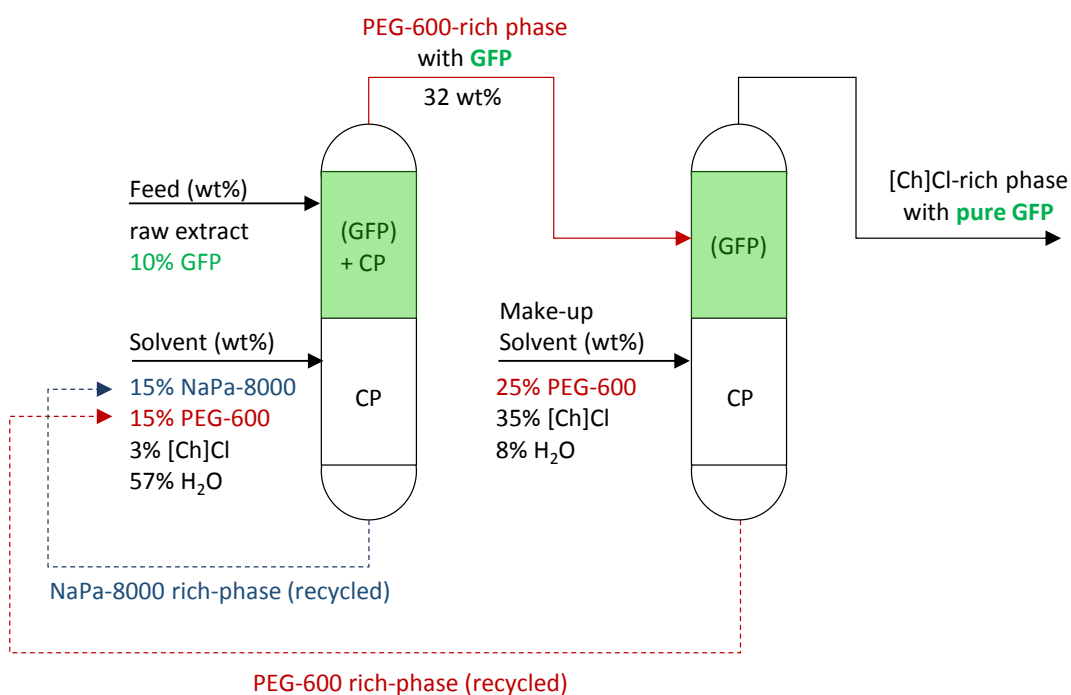


**Fig. S9.** GFP Back-extraction diagram representation showing the integration of a 1<sup>st</sup> purification using PEG-600/NaPA-8000 + [Ch]Cl-based ABS, followed by a 2<sup>nd</sup> purification step using a PEG-600/[Ch]Cl-based ABS. The  $EE_{GFP}$  (%) and  $MB_{GFP}$  (%) of each system is also presented.  $MB_{GFP}$  (%) considering the overall back-extraction process. CP acronym corresponds to contaminant proteins.

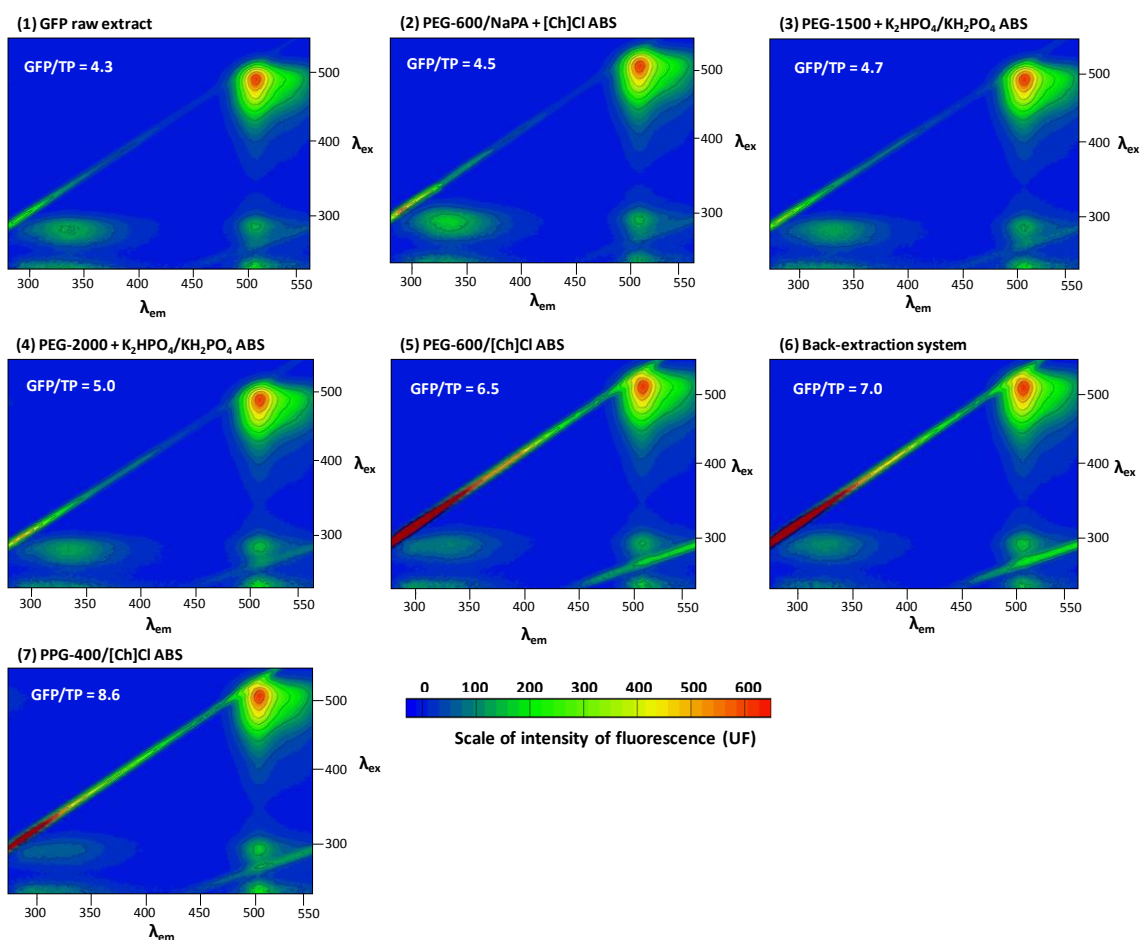


**Fig. S10.** 3D Fluorescence spectra (units of fluorescence, UF) of GFP raw extract (1) and the GFP-rich phase of the [PEG-600/NaPA-8000 + [Ch]Cl (2), PEG-1500 +  $K_2HPO_4/KH_2PO_4$  (3), PEG-2000 +  $K_2HPO_4/KH_2PO_4$  (4), PEG-600/[Ch]Cl (5), back-extraction (6) and PPG-400/[Ch]Cl (7) systems. All 3D fluorescence spectra correspond to a diluted sample with a GFP concentration of  $12.7 \pm 0.2$   $mg \cdot L^{-1}$ . The 3D Fluorescence Spectra shows the excitation wavelengths in the Y axis ( $\lambda_{ex}$ ), the emission wavelengths in the X axis ( $\lambda_{em}$ ) and the intensity of fluorescence is given by the color scale from blue to red. The GFP/TP is the ratio between the GFP and total protein fluorescence intensities (UF).

## Extraction and purification of other recombinant fluorescent proteins produced by *E. coli* using PPG-400/[Ch]Cl ABS

To evaluate if the purification aptitudes of the ABS with the highest purification yield could be applied to the extraction of other proteins, besides GFP, two other fluorescent proteins (FP) produced by *E. coli* TOP10 (Fezziwig Yellow Fluorescent Protein - YFP and Red Fluorescent Protein - RFP) were also analyzed. Both FP were kindly provided by the research group of Prof. Danielle Biscaro Pedrolli from the Department of Bioprocesses and Biotechnology, School of Pharmaceutical Sciences at São Paulo State University (UNESP). The ABS composed of 45 wt% of PPG-400 and 12 wt% of [Ch]Cl were prepared as described in **section "Extraction and purification of GFP"** of the main article (in triplicate with a blank, to subtract interferences) and evaluated by complete GFP 3D fluorescence spectra and analysis of fluorescence intensity of FP (wavelengths: YFP -  $\lambda_{ex522}$ ,  $\lambda_{em534}$ ; RFP -  $\lambda_{ex584}$ ,  $\lambda_{em610}$ ) and TP (wavelength:  $\lambda_{ex276}$ ,  $\lambda_{em336}$ ), as described in the **section "Determination of GFP 3D fluorescence spectrum and quantification of GFP and Total Protein"** of the article. The determination of the Relative Extraction for the FP ( $RE_{FP}$  (%)) and FP/TP relation (FP/TP) were given by the following equations:

$$RE_{FP}(\%) = \frac{FP_{FP-rich\ phase}}{FP_{FP-rich\ phase} + FP_{FP-poor\ phase}} \times 100 \quad \text{Equation (S6)}$$

where  $FP_{FP-rich\ phase}$  is the intensity of fluorescence of the FP in the FP rich-phase and  $FP_{FP-poor\ phase}$  is the intensity of fluorescence of the FP in the FP poor-phase;

$$FP/TP = \frac{FP_{FP-rich\ phase}}{TP_{FP-rich\ phase}} \quad \text{Equation (S7)}$$

where  $FP_{FP-rich\ phase}$  is the intensity of fluorescence of the FP in the FP rich-phase and  $TP_{FP-rich\ phase}$  is the intensity of fluorescence of the TP in the FP rich-phase.

**Table S4.** Weight fraction (wt%) and  $RE_{FP}$  (%) for extraction of YFP and RFP with PPG-400/[Ch]Cl ABS. Results correspond to the average of three independent assays and respective standard deviations.

| PPG-400/[Ch]Cl ABS | Weight fraction (wt %) |        |            | $RE_{FP}$ (%)*   |
|--------------------|------------------------|--------|------------|------------------|
|                    | PPG-400                | [Ch]Cl | FP extract |                  |
| YFP                | 45.03                  | 12.07  | 9.98       | $99.83 \pm 0.17$ |
| RFP                | 45.08                  | 12.07  | 10.04      | $99.9 \pm 0.07$  |

\*Extraction in the [Ch]Cl rich-phase.

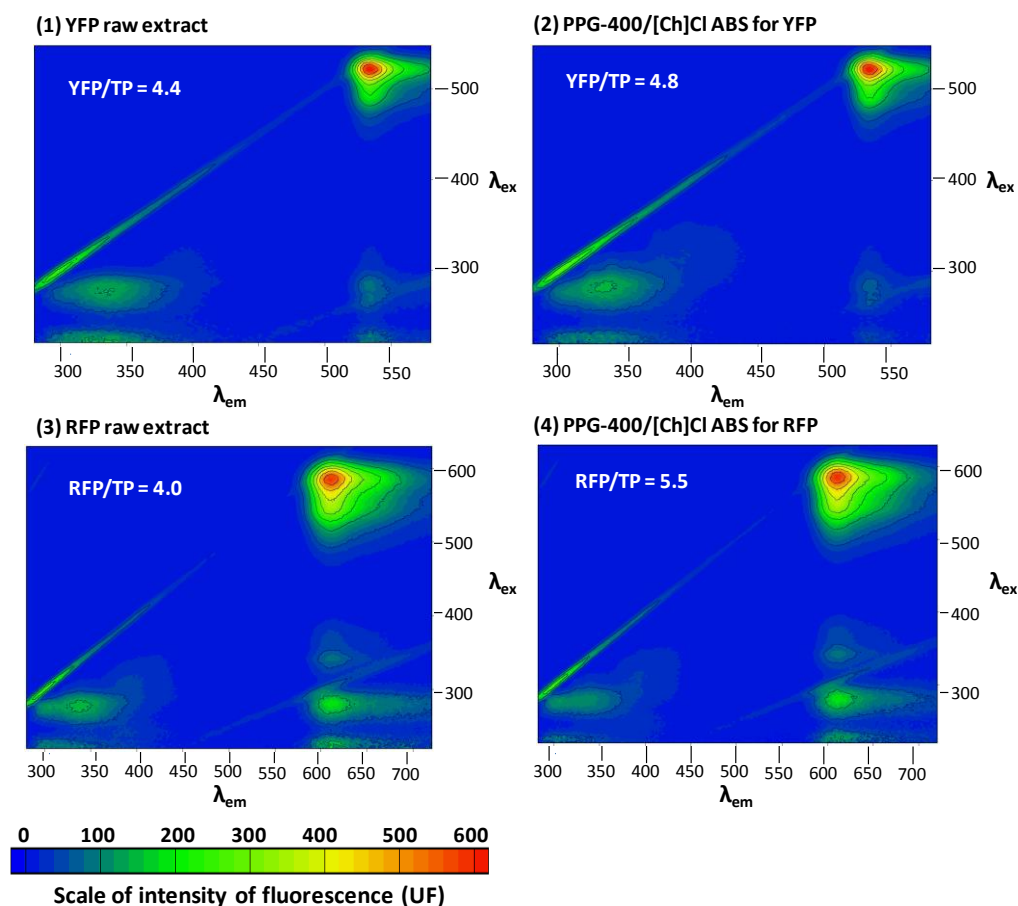


**Fig. S11.** 3D Fluorescence spectra (units of fluorescence, UF) of YFP raw extract (1) and RFP raw extract (3) and FP-rich phase of the PEG-600/[Ch]Cl ABS for the purification of YFP (2) and RFP (4). All 3D fluorescence spectra correspond to a diluted sample to present the same intensity of fluorescence in the peak of each FP ( $600 \pm 8$  UF). The 3D Fluorescence Spectra shows the excitation wavelengths in the Y axis ( $\lambda_{ex}$ ), the emission wavelengths in the X axis ( $\lambda_{em}$ ) and the intensity of fluorescence is given by the color scale from blue to red. The FP/TP relation (FP being YFP or RFP) is the ratio between the FP and total protein fluorescence intensities (UF).



## Recycling of the ABS phase former components and GFP polishing

**Table S5.** Weight (g) of the recovered top and bottom phases after the ultrafiltration of the PPG-400/[Ch]Cl ABS phases; total mass of the PPG-400/[Ch]Cl ABS before and after the solvent recycling process, with the respective recovery percentage (wt%).

| ABS                   | Weight (g)  |  |                       |
|-----------------------|---|--|-----------------------|
|                       | <b>Mass of each phase recovered after ultrafiltration</b> |  |                       |
|                       | <b>PPG-400-rich phase (top)</b>                           | <b>[Ch]Cl-rich phase* (bottom)</b>           |                       |
|                       | $3.5667 \pm 0.0587$                                       | $6.0282 \pm 0.1015$                          |                       |
|                       | <b>Total mass of the ABS before recycling</b>             | <b>Total mass of the ABS after recycling</b> | <b>Recovery (wt%)</b> |
| <b>PPG-400/[Ch]Cl</b> | $10.0203 \pm 0.0129$                                      | $6.7685 \pm 0.2480$                          | $60.7 \pm 2.2$        |

\*Not all the content of the bottom phase was used in the formation of the recycled ABS;  $2.5205 \pm 0.2346$  g of the recovered bottom phase was added in  $3.5667 \pm 0.0587$  g of the recycled top phase until the formation of a new ABS.

## References

1. de Souza, R. L.; Campos, V. C.; Ventura, S. P.; Soares, C. M.; Coutinho, J. A.; Lima, Á. S., Effect of ionic liquids as adjuvants on PEG-based ABS formation and the extraction of two probe dyes. *Fluid Phase Equilib* **2014**, *375*, 30-36, DOI 10.1016/j.fluid.2014.04.011.
2. Pereira, J. F.; Vicente, F.; Santos-Ebinuma, V. C.; Araújo, J. M.; Pessoa, A.; Freire, M. G.; Coutinho, J. A., Extraction of tetracycline from fermentation broth using aqueous two-phase systems composed of polyethylene glycol and cholinium-based salts. *Process Biochem* **2013**, *48* (4), 716-722, DOI 10.1016/j.procbio.2013.02.025.
3. Quental, M. V.; Caban, M.; Pereira, M. M.; Stepnowski, P.; Coutinho, J. A.; Freire, M. G., Enhanced extraction of proteins using cholinium-based ionic liquids as phase-forming components of aqueous biphasic systems. *Biotechnol J* **2015**, *10* (9), 1457-1466, DOI 10.1002/biot.201500003.
4. ExPASy, ProtScale. <https://web.expasy.org/protscale> (accessed 11 April 2018).
5. iGEM, Registry of standard biological parts: BBa\_K1094400: Enhanced Green Fluorescent Protein (eGFP). [http://parts.igem.org/Part:BBa\\_K1094400](http://parts.igem.org/Part:BBa_K1094400) (accessed 11 April 2018).
6. Ishihama, Y.; Schmidt, T.; Rappsilber, J.; Mann, M.; Hartl, F. U.; Kerner, M. J.; Frishman, D., Protein abundance profiling of the *Escherichia coli* cytosol. *BMC genomics* **2008**, *9* (1), 102, DOI 10.1186/1471-2164-9-102.
7. Sambrook, J.; Russell, D. W., Molecular cloning: a laboratory manual 3<sup>rd</sup> edition. *Coldspring-Harbour Laboratory Press, UK* **2001**.
8. Pereira, J. F.; Lima, Á. S.; Freire, M. G.; Coutinho, J. A., Ionic liquids as adjuvants for the tailored extraction of biomolecules in aqueous biphasic systems. *Green Chem* **2010**, *12* (9), 1661-1669, DOI 10.1039/C003578E.
9. Merchuk, J. C.; Andrews, B. A.; Asenjo, J. A., Aqueous two-phase systems for protein separation: studies on phase inversion. *J Chromatogr B Biomed Sci Appl* **1998**, *711* (1), 285-293, DOI 10.1016/S0378-4347(97)00594-X.